Supplementary Information for:

Criegee Intermediates React with Ozone

Henrik G. Kjaergaard[1,], Theo Kurtén[2], Lasse B. Nielsen[1], Solvejg Jørgensen[1], Paul O. Wennberg[3,4]*

[1]Department of Chemistry, University of Copenhagen, Universitetsparken 5, DK-2100 Copenhagen Ø, Denmark

[2]Laboratory of Physical Chemistry, Department of Chemistry, P.O. BOX 55, University of Helsinki, FI-00014, Finland.

[3]Division of Engineering and Applied Science, California Institute of Technology, Pasadena, CA 91125, USA

[4]Division of Geological and Planetary Sciences, California Institute of Technology, Pasadena, CA 91125, USA.

CORRESPONDING AUTHOR FOOTNOTE: To whom correspondence should be addressed. E-mail: hgk@chem.ku.dk. Fax: 45-35320322. Tel.: 45-35320334.

TABLE S1: The absolute energies (Hartree) and relative zero point vibrational energy (ZPVE, in kcal/mol) for the reaction between H_2COO and O_3.

Geometry	UB3LYP/aVTZ					UHF-UCCSD(T)/VDZ	
Compound	B3LYP[a]	ZPVE[a]	F12[b]	UCCSD(T)[c]	RCCSD(T)[d]	UCCSD(T) /VDZ[e]	UCCSD(T) / aVTZ[f]
H_2COO+O_3	-415.16814	0.0	-414.59161	-414.48413	-414.48430	-414.03025	-414.48474
RAO5	-415.23843	4.1	-414.66489	-414.56051	-414.56051	-414.10105	-414.56013
SP2	-415.22577	2.7	-414.65297	-414.53800	-414.54831	-414.08666	-414.53706
RIO3 + O_2	-415.26247	-1.2	-414.66434	-414.56086	-414.56081	-414.11921	-414.56175
SP3 + O_2	-415.25986	-1.7	-414.64666	-414.55371	-414.55364	-414.10807	-414.54997
H_2CO + 2 O_2	-415.32138	-2.8	-414.72995	-414.62464	-414.62458	-414.19069	-414.62455

[a]UB3LYP/aug-cc-pVTZ calculation at its optimized geometry. Harmonic zero point vibrational energy relative to that of the reactants $H_2COO + O_3$.

[b]RHF-UCCSD(T)-F12a/VDZ-F12 single point energy calculated at the UB3LYP/aug-cc-pVTZ optimized geometry.

[c]UHF-UCCSD(T)/aug-cc-pVTZ single point energy calculated at the UB3LYP/aug-cc-pVTZ optimized geometry.

[d]RHF-RCCSD(T)/aug-cc-pVTZ single point energy calculated at the UB3LYP/aug-cc-pVTZ optimized geometry.

[e]UHF-UCCSD(T)/cc-pVDZ optimized geometry.

[f]UHF-UCCSD(T)/aug-cc-pVTZ single point at the UHF-UCCSD(T)/cc-pVDZ optimized geometry.

TABLE S2: The T1 diagnostic values for the reaction between H_2COO and O_3.

Method	**CI**	**O_3**	**RAO5**	**SP2**	**RIO3**	**O_2**	**SP3**	**H_2CO**
F12[a]	0.042	0.027	0.019	0.029	0.037	0.014	0.116	0.015
UCCSD(T)[b]	0.043	0.060	0.020	0.040	0.030	0.018	0.033	0.015
UCCSD(T)/VDZ[c]	0.052	0.078	0.019	0.043	0.029	0.013	0.054	0.017

[a]RHF-UCCSD(T)-F12a/VDZ-F12 single point energy calculated on the UB3LYP/aug-cc-pVTZ optimized geometry.

[b]UHF-UCCSD(T)/aug-cc-pVTZ single point energy calculated on the UB3LYP/aug-cc-pVTZ optimized geometry.

[c]UHF-UCCSD(T)/cc-pVDZ optimized geometry

TABLE S3: The expectation values of the total spin $<S^2>$ before and after spin annihilation for the reaction between H_2COO and O_3.

Method	**Annihilation**	**CI**	**O_3**	**RAO5**	**SP2**	**RIO3**	**O_2**	**SP3**	**H_2CO**
UB3LYP[a]	Before	0.00	0.00	0.00	0.32	2.01	2.01	2.01	0.00
	After	0.00	0.00	0.00	0.01	2.00	2.00	2.00	0.00
UCCSD(T)[b]	Before	0.00	0.29	0.00	0.87	2.02	2.03	2.02	0.00
	After	0.00	0.02	0.00	0.12	2.00	2.00	2.00	0.00

[a]UB3LYP/aug-cc-pVTZ optimized geometry.

[b]UHF-UCCSD(T)/cc-pVDZ optimized geometry

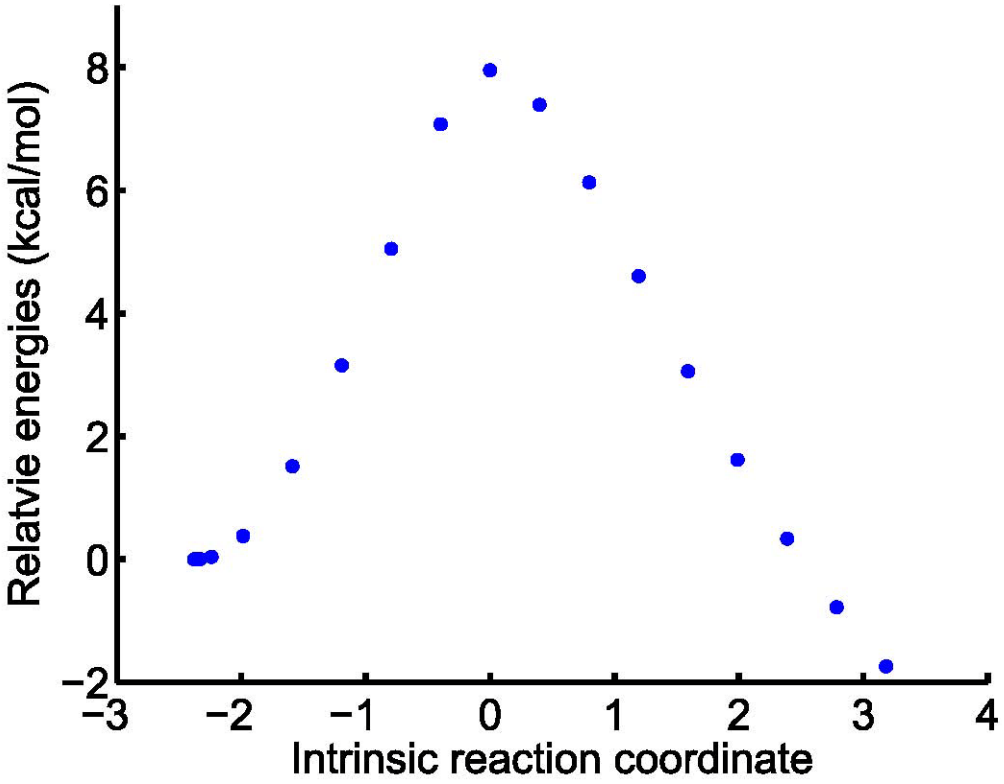

Figure S1. IRC path for the RAO5 to RIO3 + O_2 reaction. Energy is relative to energy of RAO5. The IRC path is calculated from the SP2 with the UB3LYP/aug-cc-pVTZ method without zero point vibrational energy correction.

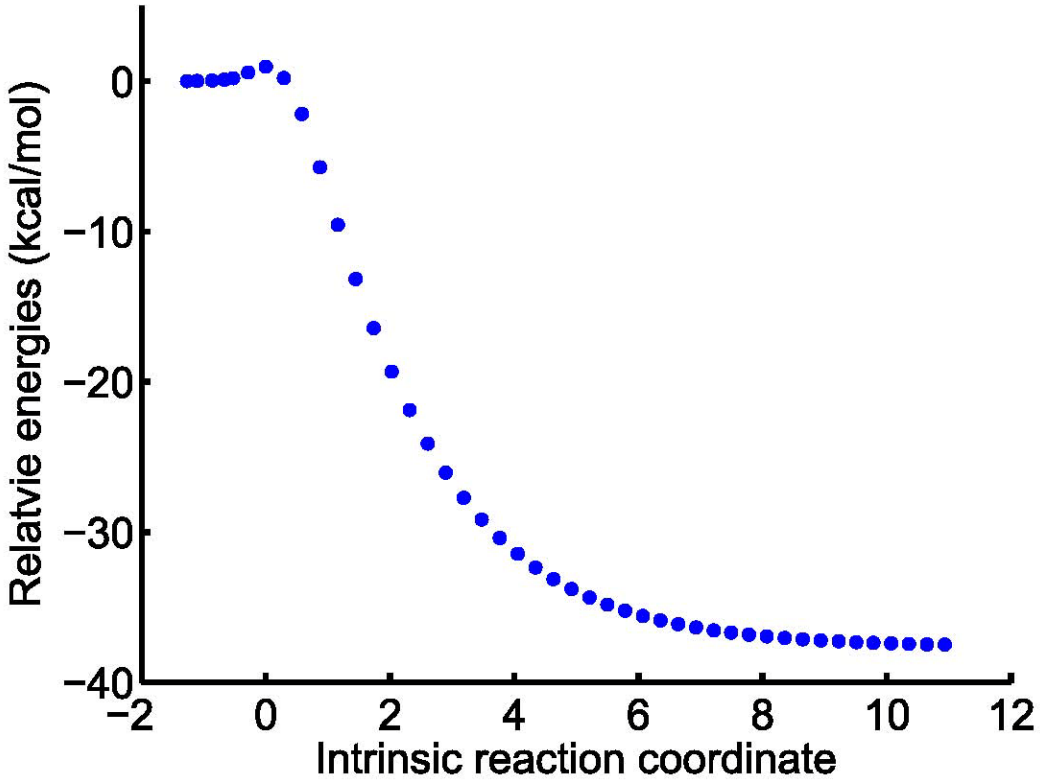

Figure S2. IRC path for the RIO3 to HCHO + O_2 reaction. Energy is relative to energy of RIO3. The IRC path is calculated from the SP3 with the UB3LYP/aug-cc-pVTZ method without zero point vibrational energy correction.

Reaction Kinetics

The reaction mechanism for the reaction between H_2COO and O_3 is sketched in Figure 2. The reaction mechanism consists of the following three elementary reactions:

Step 1: $H_2COO + O_3 \leftrightarrow RAO5$

Step 2: $RAO5 \leftrightarrow {}^3RIO3 + {}^3O_2$

Step 3: $RIO3 \leftrightarrow H_2CO + {}^3O_2$

A forward rate constant (k_i) and reverse rate constant (k_{-i}) are associated with each of the elementary reaction step. Based on the relative energies in the reaction path shown in Figure 2 of the manuscript, the overall reaction rate is likely to depend only on the rate constant of the step 1, k_1. We have estimated the rate constants for the individual steps to investigate this.

We have calculated k_2 and k_3 with RRKM-master equations in Multiwell Program Suite 2012.1 with the following parameters. Egrain1 = 10.0 cm^{-1}, imax1 = 400 cm^{-1}, Emax2 = 500 cm^{-1}, Isize = 50000 cm^{-1}, Trials = 10 mill. at 298 K, 1 atm.[1-3] Tunneling effects have been neglected, while quasi-diatomic centrifugal corrections have been applied (CENT1). Collision activation and deactivation is included according to the generalized exponential model for toluene, with α (E) = 0.1243 kcal/mol + 0.0042E and γ = 0.7.[1, 4] A thermal energy distribution (THERMAL) with an initial energy offset of 0 (EINIT) was used as the initial energy in the calculation of k_3. k_2 was calculated in the same manner with EINIT = 43.8 kcal/mol (The energy difference between the free reactants and RAO5, UCCSD(T)/aug-cc-pVTZ energies and UB3LYP/aug-cc-pVTZ zero point vibrational energy correction).

We have estimated the equilibrium constants for the first and second step, and we get K_1 = 2.0×10^{23} (ΔG = -31.8 kcal/mol) and K_2 = 2.6×10^{13} (ΔG = -18.2 kcal/mol), respectively with the program Thermo, which is a part of the Multiwell program suite. We have also calculated the pseudo first order rate constant $k_2[O_2]$ assuming an atmospheric oxygen concentration of 5.2×10^{18} molec cm^{-3}.

Assuming steady state, we can determine the rate constant k_{-1} from the equilibrium constant of the first step

$$K_i = \frac{k_1}{k_{-1}} = \exp(-\Delta G / RT)$$

where ΔG is the difference in Gibbs free energy between the reactant complex and the individual reactants and R is the gas phase constant. To ensure that K_i becomes dimensionless, we have multiplied the bimolecular constant with ρ which is the density of air at standard pressure. Based on the Multiwell (Thermo) calculated K_1 value this means that the forward reactions is significantly faster, by a factor of ca. 8000, than the reverse reaction. These rate constants are listed in Table S4 and support that the overall reaction rate is determined by k_1.

Table S4: The rate constants of the elementary reactions of the H_2COO and O_3 reaction.

Rate	k_2 **(s^{-1})**	$k_{-2}[O_2]$[b] **(s^{-1})**	k_3 **(s^{-1})**
UCCSD(T)[a]	5.5×10^{11}	4.4×10^{-3}	3.0×10^{5}

[a]Calculated with UHF-UCCSD(T)/aug-cc-pVTZ//UB3LYP/aug-cc-pVTZ energies and UB3LYP/aug-cc-pVTZ optimized geometry and frequencies.

[b]The concentration of O_2 is 5.2×10^{18} molec cm^{-3}.

We assume that the formations of RAO5 and ^{3}RIO3 are reversible but that the formation of H_2CO and $^3O_2$ from RIO3 is irreversible since the energy barrier for the reverse reaction is much higher than the forward reaction e.g $k_{-3} << k_3$.The rate law for the reaction mechanism is then

$$-\frac{d[H_2COO]}{dt} = k_1[O_3][H_2COO] - k_{-1}[RAO5]$$

$$-\frac{d[RAO5]}{dt} = -k_1[O_3][H_2COO] + (k_{-1} + k_2)[RAO5] - k_{-2}[^3RIO3][^3O_2]$$

$$-\frac{d[RIO3]}{dt} = -k_2[RAO5] + k_{-2}[^3RIO3][^3O_2] + k_3[^3RIO3]$$

$$-\frac{d[H_2CO]}{dt} = -k_3[^3RIO3]$$

If we assume that the concentrations of the RAO5 and ^{3}RIO3 are in steady state then the total rate constant for the reaction H_2COO + O_3 is given by

$$k_r = \left(k_1 - \frac{k_1 k_{-1}(k_{-2}[O_2] + k_3)}{k_{-1}k_{-2}[O_2] + k_{-1}k_3 + k_2 k_3} \right) \quad (1)$$

Using Eq. 1 yields an overall rate constant k_r that is essentially equal to k_1. Also, if we assume that the recombination reaction with oxygen (k_{-2}) is unimportant, as suggested by the rates in Table S4, then the expression for k_r simplifies to.

$$k_r = k_1\left(1 - \frac{k_{-1}}{k_{-1} + k_2}\right)$$

This simple equation gives the same results as before. We conclude that the removal of sCI with ozone is determined only by k_1.

Is there a first order saddle-point SP1?

As shown in the previous section, the overall sCI + O_3 reaction rate is determined by the formation rate of the initial RAO5 adduct. This rate in turn depends on whether or not a saddle point (SP1) separating the free reactants and RAO5 exists. Such a saddle point (SP1) was found at the RB3LYP/aug-cc-pVTZ level, but not at the UB3LYP/aug-cc-pVTZ level (Figure S3). This saddle point structure is somewhat analogous to the primary ozonide formation in usual alkene + O_3 reactions, however the MOs from the CAS calculation (see later) show clear interaction between the C and O and little interaction (and long distances) between the other O atoms on the separate units. We performed geometry optimizations at higher levels of theory to try and resolve this issue. A saddle point was found at the UHF-UCCSD(T)/cc-pVDZ level ($R_{C\cdots O}$ distance of 2.31 Å and a $R_{O\cdots O}$ distance of 3.52 Å), but spin contamination at this level was absurdly large (with $\langle S^2 \rangle$ = 3.72 after annihilation), indicating that the result is completely untrustworthy. Species with biradical character are known to be difficult problems for computational methods. In the reaction leading to RAO5, two such molecules are simultaneously forming two bonds, involving a total of four partially unpaired electrons. It is therefore not surprising that even quite advanced methods such as UCCSD(T) have problems describing the interaction, and that high T1 values and high spin contamination values can occur.

In order to determine whether or not a saddle point exists, we performed multireference calculations using the CASSCF and CASPT2 methods. The number of orbitals, and the actual orbital selection, was based on an initial CISD calculation using a minimal (STO-3G) basis set. Eight of the resulting CISD natural orbitals had significantly fractional population numbers, i.e. differing by more than 0.02 from either 2 in the case of occupied orbitals, or 0 in case of virtual orbitals. (For some input geometries, strict application of the 0.02 limit would have led to the inclusion of four occupied and five virtual orbitals, i.e. 8 electrons in 9 orbitals, but based on visual inspection of the orbitals the 8,8 space was nevertheless used.) These orbitals were then selected as input guesses for a CASSCF(8,8)/STO-3G calculation. The orbitals from that calculation were then used as input for a CASSCF(8,8)/6-31G(d) calculation. This stepwise approach follows the recommendations of Veryazov et al.[5] See Figure S4 for visualizations of the orbitals. Calculations with the larger aug-cc-pVTZ basis set then further used the 6-31G(d)

orbitals as input guesses. Dynamic correlation was included using the "RSC2" multireference second order perturbation theory module in Molpro (referred to here as "CASPT2").

CASSCF(8,8) calculations using both 6-31G(d) and aug-cc-pVTZ basis sets found a saddle point similar to that found at the RB3LYP level. Initial CASPT2(8,8)/6-31G(d) calculations starting from the CASSCF SP1 geometries did not find a saddle point, and also suffered from convergence problems. However, using the RB3LYP/aug-cc-pVTZ SP1 geometry as input, and employing a level shift of 0.3, resulted in a saddle point with a $R_{C\cdots O}$ distance of 2.07 Å and a $R_{O\cdots O}$ distance of 3.63 Å, similar to the RB3LYP/aug-cc-pVTZ SP1 geometry shown in Figure S3.

Unlike CASSCF, CASPT2 includes the dynamic correlation that is important for accurately capturing the long-range interactions between molecules approaching each other. Thus, the CASPT2 result can be taken as qualitative confirmation of the existence of SP1. Unfortunately, multireference calculations are unable to consistently treat the isolated free reactants and the SP1 using the same active space. Therefore, CASSCF and CASPT2 do not yield information on the energy of the transition state relative to the free reactants (the "barrier height"). We therefore computed several higher-level single-point energies using single-reference methods at the RB3LYP/aug-cc-pVTZ geometry in order to more accurately estimate the energy of SP1 (Table S5). IRC calculations at the RB3LYP/aug-cc-pVTZ level showed that this SP1 connected the reactants ($CI+O_3$) and RAO5 with an electronic energy barrier of 0.5 kcal/mol (Table S6 and Figure S5). The CAS space required for multireference calculation on SP1 and RAO5 are likely comparable and thus energies from these can be compared better than comparison with CAS calculations of the reactants. We therefore also performed a CASPT2(8,8)/6-31G(d) optimization of the RAO5 adduct (with symmetry switched off, and with orbital selection and level shifting as described above). We then performed CASPT2(8,8)/aug-cc-pVTZ single-point energy calculations on both the SP1 and RAO5 structures optimized at the CASPT2(8,8)/6-31G(d) level. The CASPT2(8,8) energy difference between RAO5 and SP1 was 46.4 kcal/mol using the 6-31G(d) basis set, and 43.5 kcal/mol using the aug-cc-pVTZ basis set. These values are very similar to the energy differences between RAO5 and the isolated reactants obtained using various single-reference methods (between 44 and 48 kcal/mol as shown in Table 2 of the

manuscript). The T1 diagnostics computed for RAO5 are around 0.02 (see Table S2), indicating that coupled cluster methods are reasonably reliable for this structure. This suggest barrier that the barrier height from the reactants to SP1 calculated by the single reference methods are reasonable.

In a recent study, comparing different computational methods applied to biradicals, Yang et al. found that while UCCSD(T) describes the potential energy surfaces reasonably well both close to equilibrium geometries and at long distances, it significantly overestimates energies at intermediate distances (such as those in the saddle point discussed here).[7] In contrast, both RCCSDT and UCCSDT (where the triple excitations are treated non-perturbatively) perform much better. We have therefore computed RHF-RCCSDT/cc-pVDZ energies at reactants and SP1 found at the RB3LYP/aug-cc-pVTZ level and on selected points on the RB3LYP/aVTZ IRC path (Figure S5). The energies calculated for this SP1 with the various methods are given in Table S5 and S6, and yield barrier heights between 0.5 and 4 kcal/mol with respect to the electronic energy and 12 and 15.5 kcal/mol with respect to the Gibbs free energy at 298 K and 1 atm).

We have estimated the reaction rate constant with conventional transition state theory using the rigid rotor harmonic approximation and we have not included any quantum tunneling effects. The upper limit to the barrier of 4 kcal/mol yields a reaction rate constant of 10^{-18} cm^3 $molecule^{-1}$ s^{-1} (see table S6), which can be considered an lower limit on the rate constant for the H_2COO + O_3 reaction. This rate is highly dependent on more accurate calculations for the potential SP1 followed by more accurate rate calculation. Based on our results, we suggest that a more precise determination of the size of the potential energy surface and the barrier height would require large scale multi reference calculation likely with a full valence active space, such that reactant and SP1 energies can be compared. With an accurate potential energy curve, the conventional TST calculation could then be improved with a more precise reaction rate calculation with variational TST methods.[8-9] If SP1 does not exist, then the rate constant could be determined with use of the large CAS multireference potential and more advanced kinetics methods like the variable reaction coordinate transition state theory (VRC-TST).[10-13]

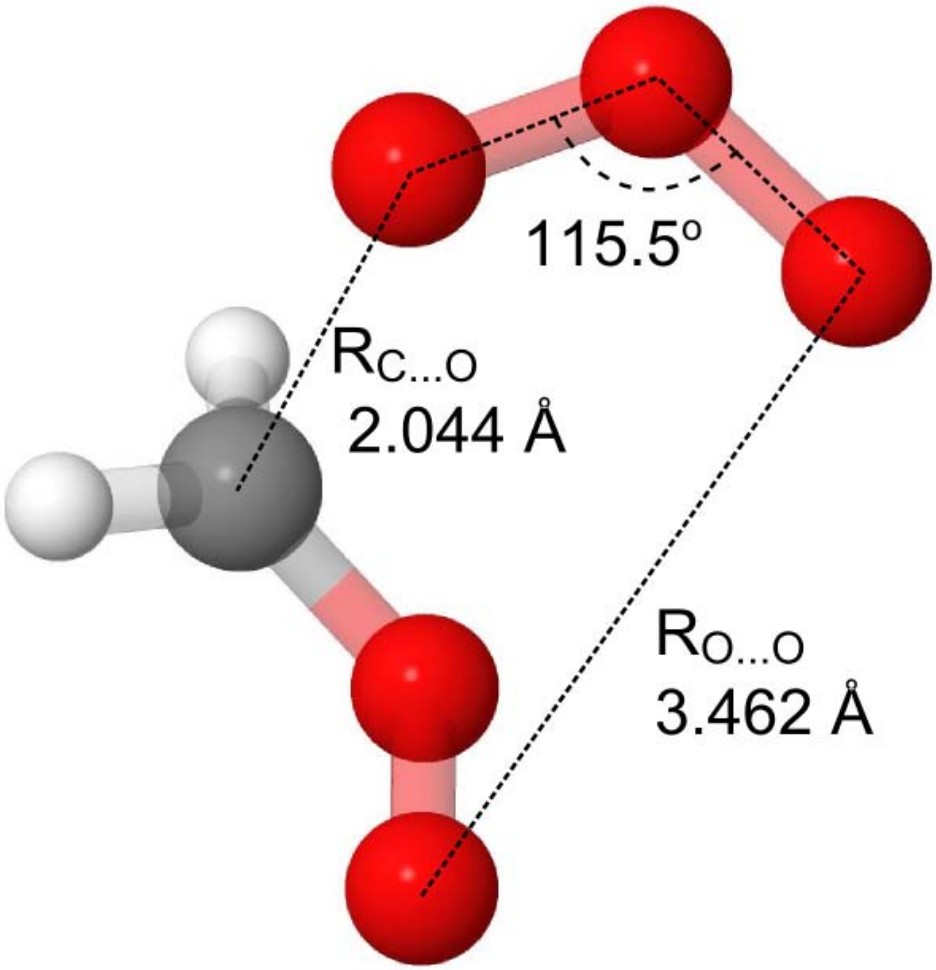

Figure S3. The structure of SP1 optimized with RB3LYP/aug-cc-pVTZ level of theory. The distance to the middle O atom in H_2COO from the right most O atom in O_3 is 2.86Å.

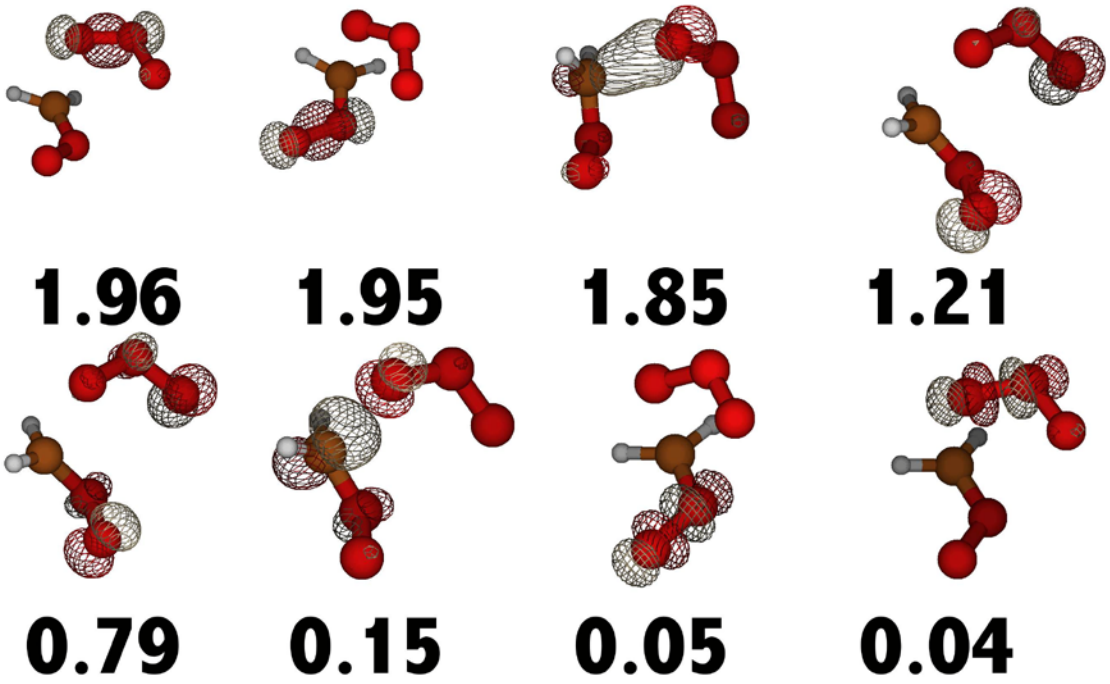

Figure S4. The 0.1 a.u. isosurfaces of the CASSCF(8,8)/6-31G(d) orbitals of SP1, at the CASPT2(8,8)/6-31G(d) optimized geometry (level shift of 0.3). CASSCF(8,8)/6-31G(d) natural occupation numbers are given below each orbital. The occupation numbers of the initial CISD/STO-3G orbitals used as input guess were 1.973, 1.966, 1.928, 1.866, 0.159, 0.091, 0.039 and 0.029, respectively. The active space encompasses both the C…O and O…O interactions between the two reactants, as well as the O-O bonds within in both reactants. The occupied and virtual orbitals also present clear bonding-antibonding pairs.

TABLE S5: The absolute energies (E) and zero point vibrational energies (ZPVE) in Hartree, the expectation of the total spin value ($<S^2>$) before and after annihilation, and the T1 diagnostic values for SP1 in the reaction between H_2COO and O_3.

Method	**Molec.**	**E**	**ZPVE**	**$<S^2>$** Before	**$<S^2>$** After	**T1**
Geometry optimization RB3LYP/aug-cc-pVTZ[c]	SP1	-415.16735	0.04048	-	-	-
	O_3	-225.50555	0.00725	-	-	-
	CI	-189.66259	0.03107	-	-	-
Single point RHF-UCCSD(T)-F12A/VDZ-F12	SP1[a]	-414.58681	-	-	-	0.05
	O_3[a]	-225.21046	-	-	-	0.03
	CI[a]	-189.38114	-	-	-	0.04
Single point UHF-UCCSD(T)/aug-cc-pVTZ	SP1[a]	-414.47041	-	1.51	2.96	0.06
	O_3[a]	-225.15262	-	0.00	0.00	0.06
	CI[a]	-189.33151	-	0.00	0.00	0.04
Single point RHF-RCCSD(T)/aug-cc-pVTZ	SP1[a]	-414.48093	-	-	-	0.05
	O_3[a]	-225.15279	-	-	-	0.03
	CI[a]	-189.33151	-	-	-	0.04
Single point RHF-RCCSDT/cc-pVDZ	SP1[a]	-414.02174	-	-	-	-
	O_3[a]	-224.90823	-	-	-	-
	CI[a]	-189.11979	-	-	-	-
Geometry optimization UHF-UCCSD(T)/cc-pVDZ	SP1	-414.01228	0.03762	1.76	3.72	0.06
	O_3	-224.90955	-	0.29	0.02	0.08
	CI	-189.12070	-	0.00	0.00	0.05
Geometry optimization RHF-RCCSD(T)/cc-pVDZ	SP1	-414.02582	-	-	-	0.06
	O_3	-224.90970	-	-	-	0.03
	CI	-189.12070	-	-	-	0.05
Geometry optimization CASSCF/aug-cc-pVTZ	SP1	-413.16941	-	-	-	-
	RAO5	-413.28694				
Geometry optimization CASPT2/6-31G(d)	SP1	-413.87732	-	-	-	-
	RAO5	-413.95123				
Geometry optimization CASPT2/aug-cc-pVTZ	SP1	-414.40310	-	-	-	-
	RAO5	-414.47238				

[a]Calculated at RB3LYP/aug-cc-pVTZ optimized geometry. For CI and O_3 UB3LYP and RB3LYP give the same energy.

TABLE S6: The SP1 barrier height (in kcal/mol) for the reaction between H_2COO and O_3.

Method[a]	**ΔE**	**ΔE_{ZPVE}** [b]	**ΔG** [c]	**k** [d] **(cm^3 $molc.^{-1}$ s^{-1})**
RB3LYP/aug-cc-pVTZ	0.50	1.85	12.01	3.98×10^{-16}
RHF-RCCSD(T)/aug-cc-pVTZ	2.12	3.47	13.62	2.60×10^{-17}
RHF-UCCSD(T)-F12A /VDZ-F12	3.01	4.36	14.52	5.73×10^{-18}
RHF-RCCSDT/ cc-pVDZ	3.94	5.29	15.45	1.19×10^{-18}

[a]All calculated at the RB3LYP/aug-cc-pVTZ optimized geometry.
[b]Electronic energy including zero point vibrational energy calculated with the RB3LYP/aug-cc-pVTZ method.
[c] Thermal corrections from the RB3LYP/aug-cc-pVTZ results.
[d]Rate constant calculated with conventional TST with the ΔG values.

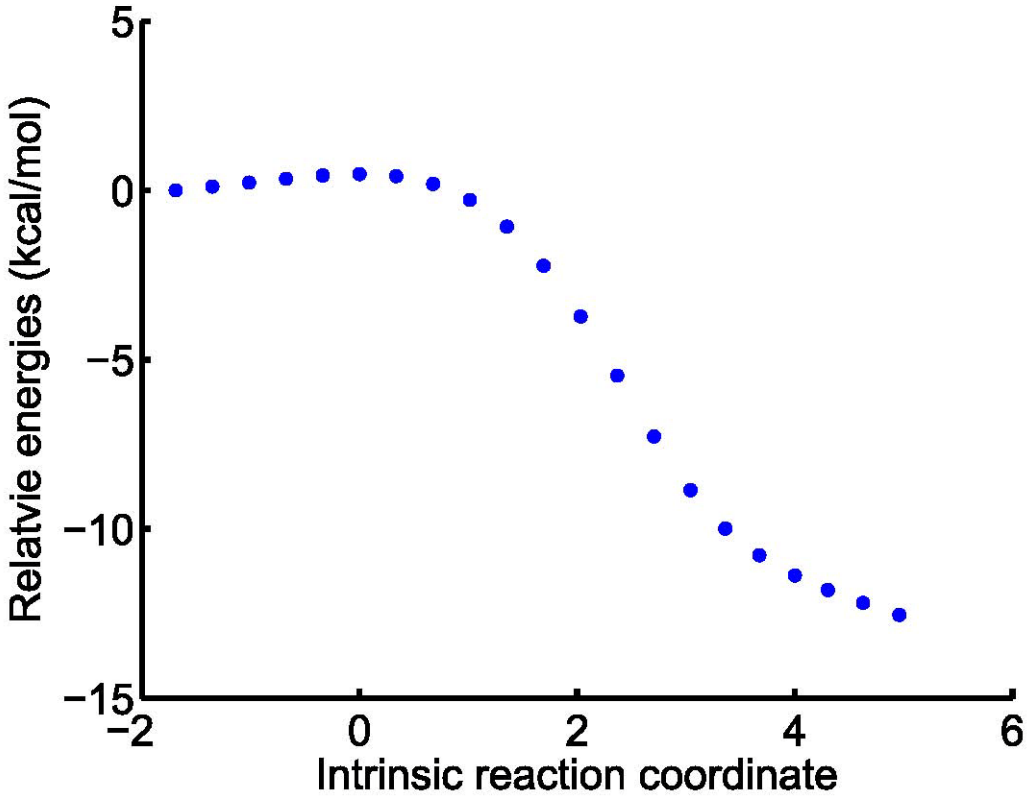

Figure S5. IRC path for the $H_2COO + O_3$ to RAO5 reaction. Energy is relative to energy of the reactants $H_2COO + O_3$. The reaction path is calculated from the SP1 with the RB3LYP/aug-cc-pVTZ method without zero point vibrational energy correction.

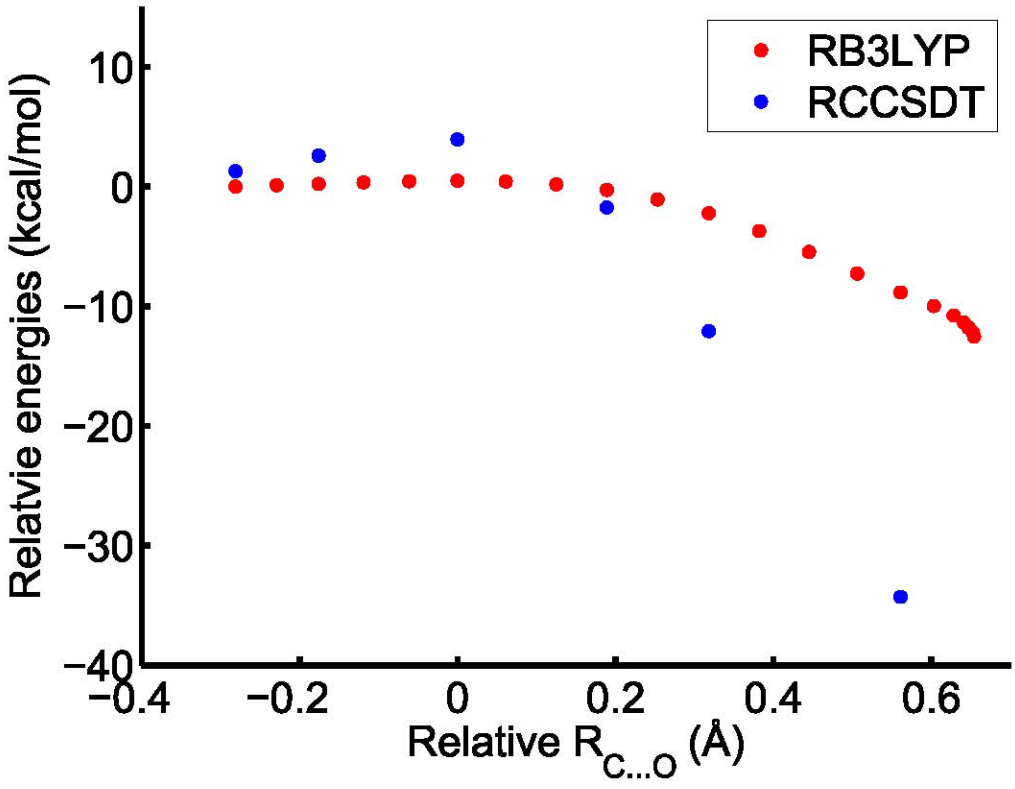

Figure S6. CCSDT/cc-pVDZ single points energies on selected points on the RB3LYP/aug-cc-pVTZ IRC of SP1 connecting reactants ($CI+O_3$) and products (RAO5). The coordinate is the difference in the $R_{C..O}$ distance relative to the $R_{C..O}$ in SP1optimized with the RB3LYP/aug-cc-pVTZ method.

TABLE S7: The harmonic and anharmonic vibrational frequencies as well as the IR intensities from the harmonic calculation for H_2COO with the UB3LYP/aug-cc-pVTZ method.

Mode	Harmonic Frequencies (cm^{-1})	IR Intenensity (harmonic) (km/mol)	Anharmonic Frequencies (cm^{-1})
1	527.2	0.09	517.6
2	672.8	4.58	658.4
3	912.2	105.7	889.7
4	949.5	30.7	938.4
5	1242.0	18.0	1219.8
6	1401.6	16.4	1372.8
7	1542.6	30.6	1543.9
8	3120.9	3.09	3005.1
9	3721.0	0.50	3123.2

TABLE S8: The harmonic and anharmonic vibrational frequencies as well as the IR intensities from the harmonic calculation for O_3 with the UB3LYP/aug-cc-pVTZ method.

Mode	Harmonic Frequencies (cm^{-1})	IR Intenensity (harmonic) (km/mol)	Anharmonic Frequencies (cm^{-1})
1	745.8	5.34	735.5
2	1188.7	234.6	1167.2
3	1248.8	0.00	1229.4

TABLE S9: The harmonic and anharmonic vibrational frequencies as well as the IR intensities from the harmonic calculation for RAO5 with the UB3LYP/aug-cc-pVTZ method.

Mode	Harmonic Frequencies (cm^{-1})	IR Intenensity (harmonic) (km/mol)	Anharmonic Frequencies (cm^{-1})
1	347.0	5.01	342.1
2	367.2	7.56	360.9
3	498.4	0.00	480.3
4	525.4	1.95	479.1
5	555.1	4.12	546.8
6	578.8	2.28	566.7
7	761.6	10.8	744.5
8	825.1	9.09	803.9
9	847.7	17.8	822.7
10	924.7	4.98	860.6
11	945.5	55.5	907.8
12	1005.0	47.2	972.5
13	1159.4	4.43	1137.7
14	1290.5	0.84	1256.6
15	1385.9	1.15	1354.4
16	1461.3	3.32	1438.5
17	3055.6	22.82	2952.2
18	3136.3	3.51	2983.3

TABLE S10: The harmonic and anharmonic vibrational frequencies as well as the IR intensities from the harmonic calculation for SP1 with the RB3LYP/aug-cc-pVTZ method.

Mode	Harmonic Frequencies (cm^{-1})	IR Intenensity (harmonic) (km/mol)	Anharmonic Frequencies (cm^{-1})
1	63.3	1.28	53.0
2	108.6	3.26	100.7
3	154.4	5.78	150.5
4	276.0	5.62	268.1
5	399.2	3.71	391.1
6	530.4	1.02	518.0
7	721.2	3.57	710.1
8	842.8	1.39	843.0
9	935.5	199.6	917.4
10	977.8	36.9	962.9
11	1093.6	56.7	1078.5
12	1182.2	214.0	1163.7
13	1232.0	12.8	1207.0
14	1341.4	25.4	1205.8
15	1494.7	11.1	1463.8
16	3136.9	2.58	3034.5
17	3378.9	2.08	3121.3
18	193.3i		273.4i

Reaction of $(CH_3)_2COO + O_3$

TABLE S11: The energetic in kcal/mol for the reaction between $(CH_3)_2COO$ and O_3.

Compound	B3LYP[a]	UCCSD(T)[b]	F12[c]	ΔZPVE[d]	ΔG[e]
$(CH_3)_2COO+ O_3$	0.0	0.0	0.0	0.0	0.0
RAO5	-32.8	-40.1	-37.5	3.3	-23.8
SP2	-24.5	-26.6	-30.6	2.0	-11.8
RIO3 + O_2	-47.9	-41.7	-24.9	-0.8	-42.1
SP3 + O_2	-47.1	-38.4	-35.1	-1.7	-39.8
$(CH_3)_2CO$ + 2 O_2	-93.3	-84.1	-83.1	-2.2	-96.7

[a]UB3LYP/aug-cc-pVTZ optimized geometry.

[b]UHF-UCCSD(T)/aug-cc-pVTZ single point energy calculated at the UB3LYP/aug-cc-pVTZ optimized geometry.

[c]RHF-UCCSD(T)-F12a/VDZ-F12 single point energy calculated at the UB3LYP/aug-cc-pVTZ optimized geometry.

[d]Calculated with the UB3LYP/aug-cc-pVTZ method.

[e]Including UHF-UCCSD(T)/aug-cc-pVTZ energies and UB3LYP/aug-cc-pVTZ thermal corrections at 298.15K.

TABLE S12: The absolute energetic in Hartree for the reaction between $(CH_3)_2COO$ and O_3.

Compound	B3LYP [a]	F12[b]	UCCSD(T)[c]
$(CH_3)_2COO+O_3$	-493.85678	-493.12690	-492.99824
RAO5	-493.90902	-493.18663	-493.06207
SP2	-493.89580	-493.17567	-493.04058
RIO3 + O_2	-493.93313	-493.16651	-493.06462
SP3 + O_2	-493.93182	-493.18280	-493.05944
$(CH_3)_2CO$ + 2 O_2	-494.00544	-493.25929	-493.13231

[a]UB3LYP/aug-cc-pVTZ optimized geometry.

[b]RHF-UCCSD(T)-F12a/VDZ-F12 single point energy calculated at the UB3LYP/aug-cc-pVTZ optimized geometry.

[c]UHF-UCCSD(T)/aug-cc-pVTZ single point energy calculated at the UB3LYP/aug-cc-pVTZ optimized geometry.

TABLE S13: The T1diagnostic values for the reaction between $(CH_3)_2COO$ and O_3

Method	**$(CH_3)_2COO$**	**O_3**	**RAO5**	**SP2**	**RIO3**	**O_2**	**SP3**	**$(CH_3)_2CO$**
F12[a]	0.031	0.027	0.017	0.025	0.109	0.014	0.155	0.013
UCCSD(T) [a]	0.031	0.060	0.018	0.035	0.026	0.018	0.02	0.013

[a]RHF-UCCSD(T)-F12a/VDZ-F12 single point energy calculated on the UB3LYP/aug-cc-pVTZ optimized geometry.

[b]UHF-UCCSD(T)/aug-cc-pVTZ single point energy calculated on the UB3LYP/aug-cc-pVTZ optimized geometry.

TABLE S14: The expectation values of the total spin $<S^2>$ before and after spin annihilation for the reaction between $(CH_3)_2COO$ and O_3.

Method	**Annihilation**	**$(CH_3)_2COO$**	**O_3**	**RAO5**	**SP2**	**RIO3**	**O_2**	**SP3**	**$(CH_3)_2CO$**
UB3LYP/aug-cc-pVTZ	Before	0.00	0.00	0.00	0.33	2.01	2.01	2.01	0.00
	After	0.00	0.00	0.00	0.01	2.00	2.00	2.00	0.00

TABLE S15: The absolute energies (Hartree) and the T1 diagnostic values of the SP1 for reaction between $(CH_3)_2COO$ and O_3**.**

Compound	**RB3LYP/aug-cc-pVTZ**	**F12[a]**	**UCCSD(T) [b]**	**ZPVE[c]**
SP1	-493.84874	-493.13117	-493.00127	0.09602
T1 diagnostic	-	0.053	0.036	-

[a]RHF-UCCSD(T)-F12a/VDZ-F12 single point energy calculated on the UB3LYP/aug-cc-pVTZ optimized geometry.

[b]UHF-UCCSD(T)/aug-cc-pVTZ single point energy calculated on the UB3LYP/aug-cc-pVTZ optimized geometry.

[b]Calculated with the RB3LYP/aug-cc-pVTZ method.

XYZ-COORDINATES:

The following structures have been optimized with UB3LYP/aug-cc-pVTZ unless otherwise stated. Coordinates given in Ångstrøm.

In H_2COO path:

CI:

C	1.071837	0.201449	0.000014
H	1.978915	-0.385346	0.000091
H	1.025261	1.283232	-0.000062
O	0.005472	-0.458297	0.000043
O	-1.176367	0.197601	-0.000034

RAO5:

O	0.804116	-1.081806	0.000000
O	0.008473	-0.743322	1.125541
O	0.005289	0.699881	1.162290
C	-0.704092	1.085118	0.000000
H	-0.722454	2.173556	0.000000
H	-1.699200	0.639082	0.000000
O	0.005289	0.699881	-1.162290
O	0.008473	-0.743322	-1.125541

RAO5: CASPT2(8,8)/6-31G(d) (symmetry switched off)

O	0.818752	-1.091151	0.000000
O	-0.012447	-0.750942	1.140887
O	0.014668	0.720679	1.167689
C	-0.699186	1.084896	0.000000
H	-0.730797	2.175374	0.000000
H	-1.687315	0.620475	0.000000
O	0.014668	0.720679	-1.167689
O	-0.012447	-0.750942	-1.140887

SP2:

O	-1.182228	-0.773341	-0.301127
O	0.432120	-1.358574	0.268090
O	1.252603	-0.457907	-0.324730
C	0.949659	0.848505	0.223734
H	1.720556	1.518425	-0.156483
H	0.953499	0.765055	1.311709
O	-0.252173	1.327525	-0.268619
O	-1.299753	0.337911	0.314599

RIO3:

H	0.307368	1.232889	0.542642
C	0.590960	0.407230	-0.134849
O	1.696710	-0.202297	0.181673
O	-1.670483	0.154723	0.149841
O	-0.584224	-0.511980	-0.163328
H	0.672754	0.820753	-1.159253

SP3:

```
O        1.400241  -0.511093   0.120468
O        0.754643   0.533745  -0.242009
C       -0.778519   0.479328   0.177880
H       -1.169114   1.394777  -0.291258
H       -0.674097   0.596431   1.269254
O       -1.339007  -0.630292  -0.134207
```

RAO5open:

```
O       -1.942640  -0.107689   0.000726
O       -1.083140  -0.997540   0.566658
O        0.978292  -0.728801  -0.755045
O        1.847891  -0.286773   0.069973
O        1.745283   0.955570   0.385107
C       -1.544461   1.056042  -0.232660
H       -0.525043   1.336794   0.005600
H       -2.284711   1.705584  -0.680265
```

Formaldehyde:

```
O        0.0       0.0         0.673246
C        0.0       0.0        -0.527145
H        0.0       0.938459   -1.111551
H        0.0      -0.938459   -1.111551
```

Ozone:

```
O        0.0        0.0        0.429137
O        0.0        1.077282  -0.21457
O        0.0       -1.07728   -0.21457
```

SP1: RB3LYP/aug-cc-pVTZ

O	1.293749	-0.1998	0.506261
O	1.954956	-0.69254	-0.55942
O	-1.39556	-1.13113	0.193651
O	-1.75526	0.072862	0.060535
O	-0.93387	0.833581	-0.60303
C	0.845292	0.990375	0.391241
H	1.195679	1.599253	-0.42978
H	0.420353	1.394674	1.298344

SP1: UHF-UCCSD(T)/cc-pVDZ

O	-1.387391	-0.158975	-0.506432
O	-1.940866	-0.848745	0.494646
O	1.511129	-1.160262	-0.122770
O	1.776367	0.100522	-0.218679
O	1.082553	0.872014	0.598939
C	-1.050929	1.071621	-0.257389
H	-1.333862	1.505690	0.706827
H	-0.694903	1.628153	-1.128121

SP1: CASSCF(8,8)/aug-cc-pVTZ

O	-1.434733	-0.172594	-0.467597
O	-2.128198	-0.771022	0.490372
O	1.670922	-1.093331	-0.194773
O	1.791041	0.143295	-0.267510
O	1.080423	0.806273	0.680256
C	-0.992821	1.027238	-0.218733
H	-1.365163	1.536752	0.643918
H	-0.659372	1.533407	-1.098913

SP1: CASPT2(8,8)/6-31G(d)

O	0.026121	0.014330	0.058267
O	-0.069769	0.015539	1.354955
O	2.833351	-0.001561	-0.830085
O	2.570957	1.127277	-1.293526
O	1.832928	1.921819	-0.481156
C	-0.095558	1.164754	-0.564984
H	-0.472274	2.004914	0.002804
H	-0.187353	1.054315	-1.635797

In the $(CH_3)_2COO$ path:

CI:

C	-0.377887	0.024533	-0.000143
O	0.566968	-0.816443	-0.00019
O	1.857741	-0.326177	0.000168
C	-0.071745	1.465152	-0.000114
H	0.559079	1.693837	-0.863647
H	-0.975598	2.068314	-0.002662
H	0.554096	1.695007	0.866809
C	-1.751836	-0.54064	0.000123
H	-1.723225	-1.627287	0.000443
H	-2.301565	-0.191313	0.87769
H	-2.301651	-0.191864	-0.877656

SP1:

O	0.514121	0.813298	-0.750466
O	0.889895	1.917453	-0.092505
O	-2.08516	0.658136	-0.255154
O	-1.859798	-0.453814	0.319214
O	-0.733318	-0.476809	1.021004
C	0.752901	-0.337616	-0.14036
C	0.554474	-1.496956	-1.066185
H	0.371583	-2.405662	-0.499021
H	-0.274416	-1.312525	-1.74571
H	1.460808	-1.634454	-1.659883
C	1.777394	-0.368905	0.939101
H	2.728105	-0.042097	0.510535
H	1.520592	0.326945	1.731607
H	1.878791	-1.377461	1.330397

RAO5:

O	-1.883848	0.0	-0.377134
O	-1.232496	-1.121268	0.197426
O	0.064227	-1.164116	-0.425739
C	0.794197	0.0	0.010102
O	0.064227	1.164116	-0.425739
O	-1.232496	1.121268	0.197426
C	2.054164	0.0	-0.829686
H	2.643509	0.885846	-0.599557
H	2.64351	-0.885846	-0.599556
H	1.800735	0.0	-1.887056
C	1.041462	0.0	1.508256
H	1.612967	0.886159	1.779255
H	0.110473	0.000001	2.065714
H	1.612966	-0.88616	1.779255

SP2:

O	1.979722	-0.137178	-0.362451
O	1.055511	1.352143	0.092349
O	-0.110043	1.133285	-0.543403
C	-0.798052	-0.060499	0.013945
O	-0.055475	-1.196407	-0.352295
O	1.342029	-1.042154	0.2836
C	-2.079017	-0.150866	-0.79277
H	-2.65155	-1.021969	-0.481342
H	-2.672037	0.745819	-0.618066
H	-1.850457	-0.230044	-1.852947
C	-1.00801	0.088745	1.509456
H	-1.623824	0.964076	1.70861
H	-1.520397	-0.796731	1.881948
H	-0.065217	0.19706	2.035612

RIO3:

C	0.426065	0.000013	-0.103538
O	1.290029	-0.000307	-1.100015
O	-1.931333	0.000133	0.134289
O	-0.956567	-0.000696	-0.743372
C	0.559325	-1.288599	0.730209
H	-0.256538	-1.313072	1.448419
H	0.498731	-2.156006	0.077101
H	1.516601	-1.284199	1.244832
C	0.559019	1.289322	0.729263
H	1.516449	1.285537	1.243586
H	0.497931	2.156232	0.075548
H	-0.256657	1.314048	1.447685

SP3:

O	-1.295661	-0.153761	-1.099018
C	-0.525172	1.401616	0.55161
H	-0.394688	2.169644	-0.207901
H	-1.498926	1.531461	1.021015
H	0.254959	1.496482	1.301084
C	-0.601935	-1.161506	0.883446
H	-1.535	-1.075793	1.435083
H	-0.575536	-2.101793	0.340215
H	0.250204	-1.088909	1.558249
C	-0.490382	0.023976	-0.102218
O	1.002722	-0.183175	-0.718062
O	1.943428	0.022484	0.136483

Acetone:

O	0.000007	1.39454	0.000003
C	0.000004	0.184277	-0.000022
C	1.287733	-0.611426	-0.001185
H	1.357501	-1.206715	0.91223
H	1.303049	-1.313622	-0.837236
H	2.141354	0.057852	-0.064541
C	-1.287744	-0.611416	0.001173
H	-1.357309	-1.207223	-0.911911
H	-1.303253	-1.313132	0.837631
H	-2.141362	0.057913	0.064007

References:

1. Barker, J. R. Multiple-well, multiple-path unimolecular reaction systems. I. MultiWell computer program suite *Int. J. Chem. Kinet.* **2001,** *33*, 232-245.
2. Barker, J. R. Energy Transfer in Master Equation Simulations: A New Approach. *Int. J. Chem. Kinet.* **2009,** *41*, 748-763.
3. Barker, J. R. *MultiWell-2012.1*, MultiWell-2012.1: 2012.
4. Barker, J. R.; Ortiz, N. F. Multiple-well, multiple-path unimolecular reaction systems. II. 2-methylhexyl free radicals *Int. J. Chem. Kinet.* **2001,** *33*, 246-261.
5. Veryazov, V.; Malmqvist, P. Å.; Roos, B. O. How to Select Active Space for Multiconfigurational Quantum Chemistry? *Int. J. Quant. Chem.* **2011,** *111*, 3329-3338.
6. Kurten, T.; Donahue, N. M. MRCISD Studies of the Dissociation of Vinylhydroperoxide, CH2CHOOH: There Is a Saddle Point. *J. Phys. Chem. A* **2012,** *116*, 6823-6830.
7. Yang, K. R.; Jalan, A.; Green, W. H.; Truhlar, D. G. Which Ab Initio Wave Function Methods Are Adequate for Quantitative Calculations of the Energies of Biradicals? The Performance of Coupled-Cluster and Multi-Reference Methods Along a Single-Bond Dissociation Coordinate. *J. Chem. Theory Comput.* **2013,** *9*, 418-431.
8. Truhlar, D. G.; Garrett, B. C. Variational transition-state theory. *Annual Review of Physical Chemistry* **1984,** *35*, 159-189.
9. Truhlar, D. G.; Garrett, B. C.; Klippenstein, S. J. Current status of transition-state theory. *Journal of Physical Chemistry* **1996,** *100*, 12771-12800.
10. Georgievskii, Y.; Klippenstein, S. J. Variable reaction coordinate transition state theory: Analytic results and application to the C2H3+H -> C2H4 reaction. *J. Chem. Phys.* **2003,** *118*, 5442-5455.
11. Klippenstein, S. J. Variational optimizations in the Rice-Ramsberger-Kassel-Marcus theory calculations for unimolecular dissociations with no reverse barrier. *J. Chem. Phys.* **1992,** *96*, 367-371.
12. Klippenstein, S. J. An efficient procedure for evaluating the number of available states within a variably defined reaction coordinate framework. *J. Phys. Chem.* **1994,** *98*, 11459-11464.
13. Harding, L. B.; Klippenstein, S. J.; Jasper, A. W. Ab initio methods for reactive potential surfaces. *Phys. Chem. Chem. Phys.* **2007,** *9*, 4055-4070.